Trends in Bioinformatics

ISSN 1994-7941

science alert

ANSInet
an open access publisher
http://ansinet.com

Trends in Bioinformatics 6 (2): 25-44, 2013
ISSN 1994-7941 / DOI: 10.3923/tb.2013.25.44

Breast Cancer Specific Histone Deacetylase Inhibitors and Lead Discovery using Molecular Docking and Descriptor Study

[1]S. Sangeetha, [2]S. Ranjitha, [3]K. Murugan and [1]G. Ramesh Kumar
[1]Bioinformatics Lab, AU-KBC Research Centre, Anna University, M.I.T Campus, Chromepet Chennai, 600044, India
[2]Centre for Biotechnology, Anna University, Guindy, Chennai, 600025, India
[3]Department of Botany and Microbiology, College of Science, King Saud University, Riyadh, Saudi Arabia

Corresponding Author: G. Ramesh Kumar, Bioinformatics Lab, AU-KBC Research Centre, Anna University, MIT Campus, Chrompet, Chennai-600044, India Tel: +91-044-22234885 Fax: +91-044-22231034

ABSTRACT

Histone deacetylases 1 and 3 (HDAC1 and HDAC3) enzyme chromatin remodeling and gene transcription altering activities are implicated in tumor behavior and progression. Their inhibitors promising pre-clinical model therapeutic efficacy makes them likely anti-cancer targets for breast cancer therapeutic intervention. In this study, both natural and synthetic Histone Deacetylase Inhibitors (HDACi) were screened using *in silico* docking, molecular descriptors and pharmacophore models to design new molecules with potential HDAC1 and HDAC3 selectivity and inhibitory activity. Three dimensional (3D) homology models of HDAC1 and HDAC3 were built based on the crystal structure of human Histone deacetylase 2 (HDAC2). Lead optimization by docking several natural and synthetic compounds were carried out and compared. There are several natural HDACi available and curcumin was found to be best docked to HDAC1 and HDAC3. Through Virtual Screening (VS) top-scored compound curcumin was identified but it shows poor drug likeness property. To overcome this problem pharmacophore modeling of the curcumin based on virtual screening of (1E, 4E)-1,5-bis (3, 4-dimethoxyphenyl) penta-1, 4- dien-3-one was studied. This study was found to be best docked to HDAC1 and HDAC3 with highest binding energies -10.20 and -10.27 kcal/mol, respectively and interacts with active site of catalytic Zn^{2+} trihedrally coordinates to the side chains of amino acids. Curcumin analogue was predicted as a potential lead drug-like molecule that selectively inhibits HDAC1 and HDAC3 that may prevent the progression and pathogenesis of breast cancer.

Key words: Breast cancer, curcumin, histone deacetylase (HDAC), molecular docking, virtual screening

INTRODUCTION

Cancer is a disease characterized by uncontrolled growth of cells. Recently, a considerable increase in their global burden and cost of care is witnessed. A study was conducted by United States National Cancer Institute's (NCI) population growth says that, by 2020, medical expenditures of cancer should be reaching around $158 billion, an increase of about 27% from the year 2010 (Mariotto *et al*., 2011). There are many types of cancer, out of which breast cancer is more common in human especially women. Previous study showed that in the year 2008, out of the women cause by cancer, 23% (1.38 million) have breast cancer and 14% (458,400) leads to death

(Jemal *et al*., 2011). Several clinical studies on chemoprevention have shown that the risk among high-risk group women may be reduced considerably by using the drugs tamoxifen and raloxifene. However, administration of tamoxifen shows some threats as an increased danger for endometrial cancer (Alteri *et al*., 2011) and no beneficial effect on Estrogen Receptor (ER) negative cancers. The efficacy of Raloxifene and tamoxifen are same but both it results in histologic profile of thrombo-embdic events. Hence, now the challenge is to find new agents achieving same or better efficacy with sparingly favorable benefit to risk ratios (Oyama *et al*., 2009).

Breast carcinogenesis is associated with well-known genetic alterations including specific gene amplifications, deletions, point mutations, chromosome rearrangements and aneuploidy. Besides, epigenetic alterations resulting in aberrant gene expression are well known key contributors. An epigenetic alteration including Cytosine Phosphate Guanine (CpG) island dinucleotide methylation and chromatin structure changes may lead to tumor suppressor gene silencing and oncogene activation through post-translational modifications of histone acetylation or DNA conformation. Unlike germ line mutations, epigenetic alteration may potentially be reversed making them attractive targets for breast cancer drug investigation and treatment (Dworkin *et al*., 2009). Numbers of epigenetic modifiers are either in use or under investigation as a single agent or in combination with other systemic therapies for cancer treatment.

Histone Acetyl Transferases (HAT) acetylates the lysine residues thus producing active chromatin and histone deacetylases as another process that deacetylates lysine residues in producing silenced chromatin. The dual process of HAT and HDAC plays an important role in modulation of chromatin topology and regulation of gene transcription. HATs preferentially acetylate specific lysine substrates between nonhistone protein substrates and transcription factors, affecting DNA-binding properties and in turn, altering gene transcription. HDAC alter the ε-amino groups of lysines into neutral ε-acetamido groups and the cause altering chromatin structure and access of gene transcription (Tambunan and Wulandari, 2010). The super family of HDAC comprises 18 members that are classified into four groups (I to IV) based on sequence homologies. HDAC Class I enzymes comprises HDAC1, HDAC2, HDAC3 and HDAC8, all nuclear proteins with ubiquitous expression. The diversity of HDACs suggests their tissue or cell line dependent differential roles (Duong *et al*., 2008). The HDAC activity inhibition by specific inhibitors induces growth arrest, differentiation and apoptosis of transforming cells as well as several cancer cells. Subha and Kumar studied assessment for the identification of better HDACi class through binding energy calculations and descriptor analysis (Subha and Kumar, 2008).

In spite of many HDACi are in clinical trials, only two Suberoylanilide Hydroxamic Acid (SAHA) and Romidepsin are the therapeutic HDACi approved by US Food and Drug Administration (US FDA) for cutaneous T-cell lymphoma treatment. Combining epigenetic therapy with existing cytotoxicity and endocrine therapy would be a promising choice for breast cancer patients (Lustberg and Ramaswamy, 2011). Recent studies on HDAC class I, the HDAC1 and HDAC3 expression in breast tumors established their potential therapeutic and prognostic significance in breast cancer. Both interact either directly or indirectly with Estrogen Receptor (ER) and Progesterone Receptor (PR), as well as with p53. In addition, HDAC1 association with breast cancer susceptibility gene breast cancer 1 (BRCA1) playing an important role in breast cancer pathophysiology is well known documented (Krusche *et al*., 2005). HDAC3 represses gene expression by directly binding to the transcriptional corepressor of Silencing Mediator for Retinoid and Thyroid (SMRT) hormone receptors and nuclear receptor corepressor (N-CoR). Though the numbers of HDACi were developed, they are yet to be available in the market and are only in

clinical phases. *In silico* approach of drug discovery reduce the cost and time of drug discovery and development. Synergistic combination of pharmacophore method with other molecular modeling approaches as docking is a good strategy to give key information and further improve the response of compound activity (Yang *et al.*, 2002).

Therefore, in the present study, modeled the HDAC1 as well as HDAC3, analyzed their interaction with the known natural and synthetic HDACi including those in phase I/II clinical trials to find the apposite breast cancer specific inhibitors. The Virtual Screening (VS) resultants for HDAC1 and HDAC3, curcumin have highest binding energy and improve its drug-likeness property. Hence, the aim of present study is identification and development of best breast cancer progression preventing drug leads by selectively inhibiting HDAC1 and HDAC3.

MATERIALS AND METHODS

Homology modeling: For solving the structures of HDAC1 and HDAC3 proteins, HDAC1 comprising 482 amino acids (Genbank accession number CAG46518.1) and HDAC3 consist of 428 amino acids (Genbank accession number NP_003874.2) were obtained from the National Center for Biotechnology Information (NCBI) (Geer *et al.*, 2010). Basic Local Allignment Search Tool (BLAST) search against the protein blast (blastp), three dimensional structure of HDAC2 (PDB ID 3MAX) showing high sequence similarity with both proteins and used as a template for both proteins (Friedrich *et al.*, 2007). Modeller 9V8 was used to generate the three dimensional structure (Paramasivan *et al.*, 2011). The stereochemical quality of the constructed homology models was assessed by running the structure assessment tool PROCHECK (Laskowski *et al.*, 1993). Finally, the refined 3D structures were visualized by PyMoL Viewer (Seeliger and de Groot, 2010).

Active site prediction: The active sites of both proteins were identified by using a CASTp server (Binkowski *et al.*, 2003). It detected all the feasible pockets in the protein structure. The first pocket was chosen as the biologically most favorable active site for docking studies.

Ligand molecules: The ligand molecules comprising natural and synthetic HDACi retrieved from NCBI-PubChem (Li *et al.*, 2010) and DrugBank database (Wishart *et al.*, 2008) were used in the present study. Best compound similar structures were collected from a ChemBank database (Seiler *et al.*, 2008). The structures were drawn using ChemSketch 12.0 Software. (Osterberg and Norinder, 2001) and energy minimized by Discovery studio [http://accelrys.com/products/discovery-studio/visualization].

Molecular docking: The docking simulation was carried out by performing docking ligands to their macromolecular receptors using AutoDock 4.0 (Morris *et al.*, 1998). In the semi-flexible docking performed, the target protein was kept as rigid whereas the ligands as flexible and their torsional roots were detected. During docking, Kollman united atom charges, solvation parameters and polar hydrogens were added to the receptor PDB file. Gasteiger charge was also assigned for ligand molecule manually and the non-polar hydrogens were merged. For each ligand, 100 docking runs conformers were specified. The ligand-protein interaction images showing the type and distance of interacting atoms, pocket information or functional sites of protein interacting with the ligand molecule were viewed.

Molecular property screening: The molecular descriptors LogP, Molecular Weight (MW), number of hydrogen bond donor (DON) and acceptor (ACC) were calculated by Molinspiration

server [http://www.molinspiration.com/cgi-bin/properties]. Violation of "Lipinski's Rule of Five" (LipViol) was recorded, if LogP>4, MW>500, DON>5 and ACC>10 (Ertl, 2012). Solubility, drug-likeness and drug score were studied by Osiris molecular property prediction server [http://www.organic-chemistry.org/prog/peo/].

RESULTS AND DISCUSSION

Homology Modeling of HDAC1 and HDAC3 proteins: HDAC1and HDAC3 three dimensional structures were modeled using human HDAC2 as a template. The search was done using the Basic blastp exhibited the highest sequence similarity (94%) and E Value (0.0) between the modeled target HDAC1 and the template. HDAC3 sequence also shared 85% sequence similarity and E Value $1e^{-178}$ with the template. The local geometry of the optimized structures was revealed by Ramachandran plot. Both modeled structures show good stereochemistry (Fig. 1a, b). Three dimension (3D) modeled HDAC1 and HDAC3 PROCHECK torsion angle analysis shown that 93.1 and 91.86% of residues were in the most favored regions respectively (Fig. 2a, b). The active sites in the modeled proteins grid box with dimension of 63.71×29.05×3.780A° were used.

Virtual screening: Docking simulations were performed for 25 natural and 23 synthetic HDACi using AutoDock program. Docking study revealed each inhibitor's different affinities with the protein. The natural compound binding energy scores, interacting amino acids shown in Table 1. The natural HDACi, curcumin was found to be best docked to HDAC1 and HDAC3 with highest binding energies -10 and -10.3 kcal/mol, respectively (Fig. 3a, b) and it interacts with the active site of catalytic Zn^{2+} trihedrally coordinates to the side chains of amino acids. Only one natural HDACi approved by FDA, romidepsin shows sparingly low binding energy of -4.55 kcal/mol for HDAC1 and for HDAC3 -3.45 kcal/mol and it doesn't interact with the active

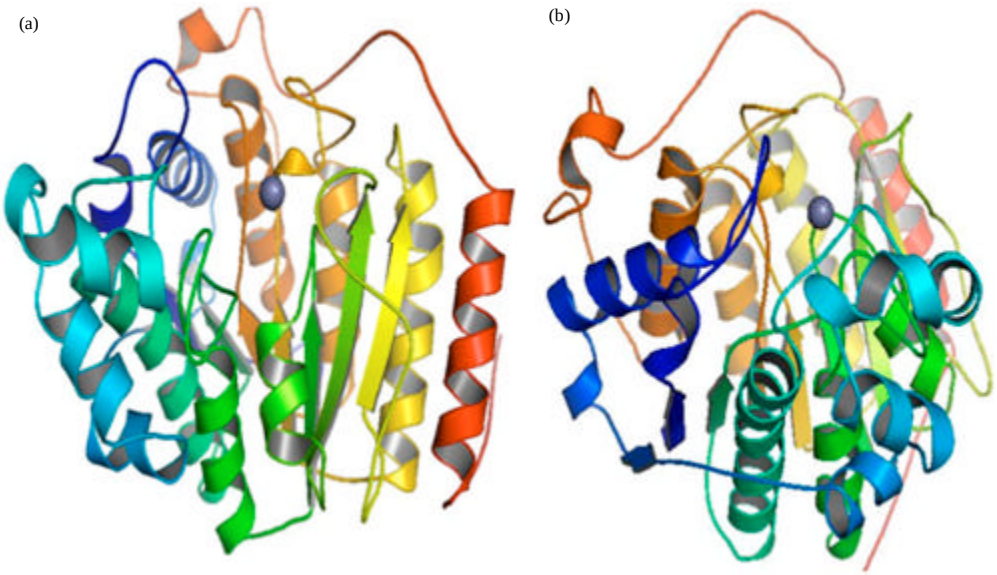

Fig. 1(a-b): Three dimensional structure of (a) Modeled histone deacetylase 1 and (b) Histone deacetylase 3 proteins, Zn (Ash) shown in sphere

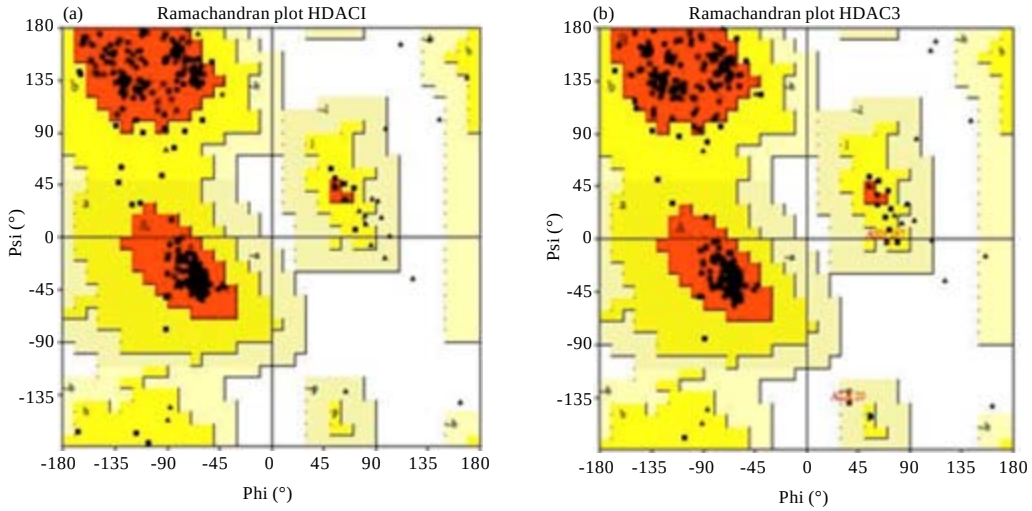

Fig. 2(a-b): Ramachandran plot statistics of (a) Histone deacetylase 1 model shows, 93.1% present in allowed regions and (b) Histone deacetylase 3 shows 91.86% of the residues in the allowed regions

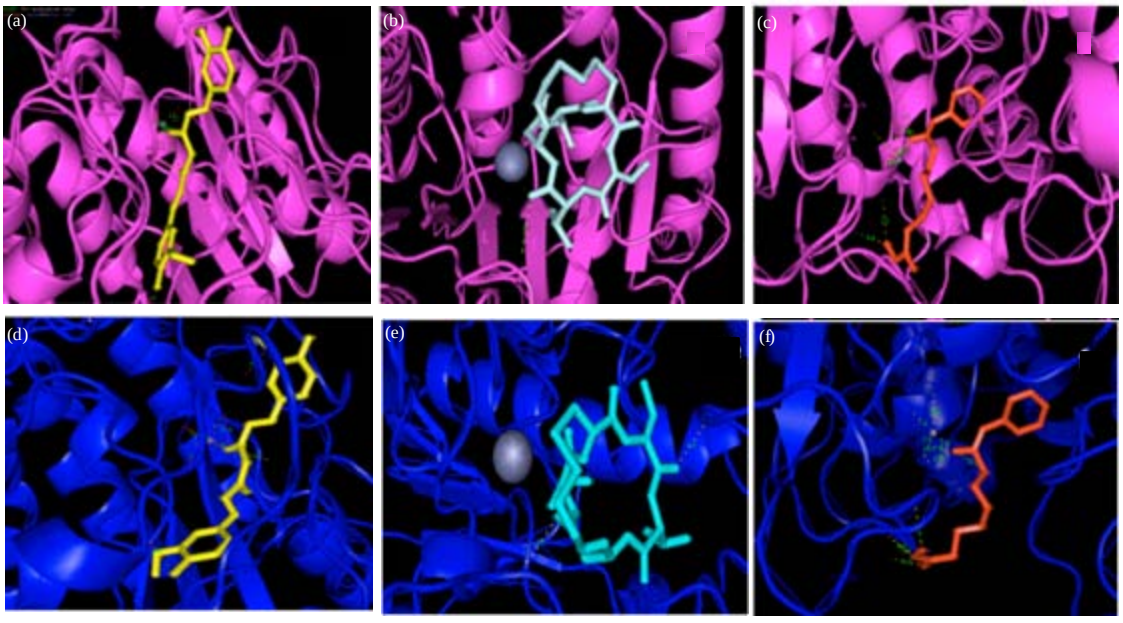

Fig. 3(a-f): Curcumin interact with (a) Histone deacetylase 1 (HDAC1) protein zinc ion is shown as sphere (ash), (b) Curcumin interact with histone deacetylase 3 (HDAC3), (c) Food and Drug administration (FDA) approved natural compound romidepsin interact with HDAC1 no interaction with zinc ion is shown as sphere, (d) Romidepsin interaction with HDAC3, (e) FDA approved suberoylanilide hydroxamic acid (SAHA) interaction with modeled HDAC1 and (f) SAHA interact with HDAC3

Table 1: Natural HDACi binding energy and interacting amino acids for HDAC1 and HDAC3

Name of the natural compound	Pubchem CID	Binding energy score (kcal/mol)		Hydrogen bonding between natural HDACi with protein interacting amino acids	
		HDAC1	HDAC3	HDAC1	HDAC3
Apicidin	467801	11.03	5.4	-	O43-His22; O35-Tyr298; O19-Asp93; O7-Leu266
Azumamide A	16095102	-8.36	-8.59	O36-His141; O36-Tyr303; O36-His178; O36-Zn; Zn-His178; Zn-Asp176, Asp176; Zn-Asp264; N37-Tyr303	O34-His172; O34-Asp170; O34-Asp259; O34-Zn; Zn-His172; Zn-Asp170; O6-His172
Azumamide D	16095113	-8.95	-8.67	O34-His140; O34-His178; O34-Asp176; O34-Zn; Zn-Asp176; Zn-Asp264; Zn-Asp178	O34-His134; O34-Asp170; O34-Asp259; O34-Zn; Zn-Asp170, Asp170; Zn-Asp259; Zn-His172
Azumamide E	16095101	-8.99	-9.22	O37-Tyr303; 037-Asp264; O37-His178; 037-Asp176; O37-Zn; Zn-Asp264; Zn-Asp176, Asp176; Zn-His178; O6-His178	O37-His172; O37-Asp170, Asp170; O37-Zn; O36-Asp259; O36-Zn; Zn-Asp170, Asp170; Zn-His172; O18-Tyr198
Benzyl iso-Thiocyanate	2346	-4.23	-4.42	-	-
Berberine	2353	-5.7	-6.37	O2-His178	O23-Tyr298; O23-Zn; Zn-Asp259; Zn-Asp170; Zn-His172
Chlamydocin	124134	-7.01	-7.55	O27-His140; 027-Asp178; O27-Asp176, Asp176; O27-Asp264; Zn-Asp264; Zn-Asp176; Zn-His178; O19-His178	O27-His135; O27-His134; O27-Asp170, Asp170; 27-Zn; Zn-His172; Zn-Asp170, Asp170; Zn-Asp259; O10-His172
Curcumin	969516	-10	-10.3	O12 -Asp264; O12-His178; O12-Zn; O15-Zn; O15- Asp176; O15-His140; Zn-Asp176, Asp176; Zn-His178; O24-Ala136	O15-Asp259; O15-His172; O15-His135; O15-Zn; Zn-Asp170, Asp170; Zn-Asp259; O2- Arg28; O27-Arg28; O12-His135
Dactinomycin	2019	3597.8	4173.55	O12-Tyr303; O12-Asp264; O15-Asp176; O15-His140; Zn-Asp176, Asp176; O15-Tyr24; O24-Ala136	O15-His172; Zn-Asp170, Asp170; O25-His172; O2-Arg28; O27-Arg28; O12-His135
Depudecin	6438725	-6.97	-7.62	O14-His178; O14-Asp264; O14-Zn; Zn-Asp176, Asp176; Zn-Asp264; Zn-His178; Zn-Tyr303; O15-AlA136; O15-Arg34	O14-Gly296; O14-Asp170; O10-His134; O14-Zn; Zn-Asp170, Asp170; Zn-Asp258, Asp259
Flavone	10680	-7.1	-8.38	O10-Gly137	O17-Tyr298; O10-His134; O10-Asp259; O10-Asp170, Asp170; O10-Zn; Zn-Asp170, Asp170; Zn-Asp259; Zn-His172
HC-toxin	107864	-7.68	-7.91	O28-His141; O28-His178; O28-Zn; O28-Asp176; Zn-Asp176, Asp176; Zn-His178; Zn-Asp264; O4-His178; O19-leu271	O28-His135; O28-Asp259; O28-Zn; Zn-His172; Zn-Asp170, Asp170; Zn-Asp259; O4-Tyr198; O4-His172
Indolocarbazole	5330716	-5.83	-6.4	N21-Asp99; N24-Asp99; O29-Gly27	O2-His135; O2-Zn; Zn-Asp170, Asp170; Zn-His172; Zn-Asp259; O29-Asp93; N27-As93
Largazole	24757913	-7.43	-5.87	O9-His178	O36-Asp93
Linoleic acid	5280450	-6.81	-8.85	O19-His140; O20-His178; O20-Tyr303; O20-Asp176; O20-Asp264; C20-Zn; Zn-His178; Zn-Asp176, Asp176; Zn-Asp264	O19-His134; O19-His135; O19-Asp170, Asp170; O19-His172; O19-Zn; O20-Zn; Zn-His172; Zn-Asp170, Asp170; Zn-Asp259; O20-His172; O20-Asp259; O20-Tyr298; -
Parthenolide	6473881	-5.58	-5.62	O16-Tyr303; O17-His178; O8-His178; O8-Tyr204	O16-Asp93
Pomiferin	4871	-6.6	-8.16	O30-Asp99; 021-Asp99; O28-Gln26	O28-Gly312; O21-Tyr298; O21-His172; O21-Zn; Zn-Hius172; Zn-Asp170, Asp170; Zn-Asp259
Psammaplin A	6400741	-9.62	-4.28	O36-His178; O22-Gly149; O22-Tyr303; O25-Gly301; O25-Gly138; O25-Gln260; O25-Asp176; N24-Asp176	O12-Gly152; O10-His135; N9-Gly142

Table 1: Continue

Name of the natural compound	Pubchem CID	Binding energy score (kcal/mol)		Hydrogen bonding between natural HDACi with protein interacting amino acids	
		HDAC1	HDAC3	HDAC1	HDAC3
Romidepsin	5352062	-4.55	-3.45	O9-Asp99	O5-Asp93; O14-leu266
Stigmasterol	5280794	-6.15	-7.17	-	-
Sulforaphane	5350	-5.46	-5.81	O3-His141; O3-Asp136; O3-His178; O3-Asp264; O3-Zn; Zn-His178; Zn-Asp264; Zn-sp176, Asp176; N8-Gly300	O3-His134; O3-His178; O3-Asp259; O3-Asp170, Asp170; O3-Zn; Zn-His172; Zn-Asp259; Zn-Asp170, Asp170
Thymoquinone	10281	-5.57	-6.78	O5-His140; 05-His141; 05-His178; O5-Asp264; O5-Zn; Zn-Asp264; Zn-Asp176, Asp176; Zn-His178	O5-His135; O5-Asp170; O5-His172; O5-Asp259; O5-Zn; Zn-His172; Zn-Asp170, Asp170; Zn-Asp259; O9-Gly93
Trapoxin A	121875	-7.08	-6.81	O41-His141; O41-His140; O41-His178; O41-Asp264; O41-Zn; Zn-His178; Zn-Asp264; Zn-Asp176, Asp176	O41-His135; O41-His134; O41-Asp170; O41-Zn; Zn-His172; Zn-Asp170, Asp170; Zn-Asp259
Trapoxin B	395803	-7.43	-5.5	O40-His141; O40-His178; O40-Tyr303; O40-Zn; Zn-Asp176, Asp176; Zn-His178; O43-Tyr303; O9-Asp99	O9-Asp93
Trichostatin A	444732	-6.89	-6.41	O11-His141; O11-His140; O11-Asp176; O11-His178; O11-Zn; Zn-His178; Zn-Asp176, Asp176; Zn-Asp264; O13-His178; O9-Gly149	O13-His172; O13-Asp170; O13-Tyr298; O13-Zn; Zn-Asp170, Asp170; Zn-His172; Zn-Asp259; O19-Tyr18; O19-phe144

HDACi: Histone deacetylase inhibitor, HADC1: Histone deacetylase 1, HDAC3: Histone deacetylase 3

site of the Zn^{2+} ion (Fig. 3c and d). Interestingly, the well known Trichostatin A (TSA) also exhibited a binding energy of -6.89 kcal/mol with HDAC1 and -6.41 kcal/mol with HDAC3. The other natural HDACi including berberine, flavones, indolocarbazole, largazole, parthenolide, pomiferin, psammaplin A, romidepsin as well as trapoxin B exhibited interaction with amino acid but not with the Zn^{2+}. Apicidin, Benzyl iso-thiocyanate and Stigmasterol not suitable for both proteins because it dosen't interact with HDAC1, for HDAC3 except apicidin, other two compounds doesn't show interaction.

Among all 23 synthetic compounds in Table 2, CRA 024781 has shown a high binding energy of -9.99 kcal/mol with HDAC1 however, it does not shown interact with the Zn^{2+}. For HDAC3, MGCD0103 showed the high binding energy of -9.86 kcal/mol. The reference standard SAHA exhibited as much close binding energy -7.28 and -7.86 kcal/mol (Fig. 3e and f) with HDAC1 and HDAC3, respectively. Trithio carbonate doesn't show interaction and Tubacin interacting with amino acids but no interaction in Zn^{2+} in both proteins. The following synthetic HDACi APHA, BML210, CI-994, CRA 024781, CUDC101, scriptaid and tubacin which were good binding energy with HDAC1 but doesn't intract with Zn^{2+}. The natural compounds Methotrexate and Pyroxamide for HDAC3 showed interaction with amino acids, dosen't show any interaction with Zn^{2+} in both the proteins.

The molecular properties of high score molecular docking hit HDACi compounds when subjected to Lipinski's screening, curcumin, trichostatin A and indolocarbazole are resulted as Lipinski positives (Table 3) among natural compounds making them potentially promising agents. The synthetic HDACi viz N-(2-aminophenyl)-4-[N-(pyridin-3-yl-methoxycarbonyl)aminomethyl]benzamide derivative (MS-275), 3-(4-dimethylaminophenyl)-N-hydroxy-2-propenamide (IN-2001), Oxamflatin, Pxd101, Scriptaid, SAHA, Dacinostat, An-9, Panobinostat (LBH-589), Phenyl butyrate, CUDC101 and N-(2-Aminophenyl)-N' phenyloctanol diamine (BML-210) are also found as non violators of Lipinski's (Table 4) parameters, compare to curcumin shows less binding energy. Even though CUDC101 and BML-210 followed the Lipinski's rule, there is no interaction with Zn^{2+}.

Out of the forty eight molecules, curcumin showed high affinity with both proteins. The catalytic Zn^{2+} trihedrally coordinates to the side chains of amino acids, interacts through hydrogen bonds and satisfies the Lipinski's rule. However, curcumin showed poor drug-likeness and necessitates generation of their analogues for overcoming this hitch and improvement of their drug-likeness property. Based on pharmacophore model, thirteen different analogues of curcumin were retrieved from ChemBank database. Thirteen analogue compounds binding energies and interacting amino acids are in Table 5, out of 13 analogue compound (1E,4E)-1,5-bis(3,4-dimethoxyphenyl)penta-1,4-dien-3-one secures high binding energy of -10.20 and -10.27 kcal/mol for HDAC1 and HDAC3, respectively. Physicochemical properties (Table 6) were calculated for 13 analogue compounds; interestingly all satisfies the Lipinski's rule. Further study of drug likeness and drug score (Table 7) property, only three compounds satisfy, they are (2E, 6E) -2, 6-bis (3, 4-dimethoxybenzylidene) cyclohexanone, (1E, 4E) -1, 5-bis (3,4-dimethoxyphenyl) penta-1, 4-dien-3-one and (2E,5E) -2, 5-bis (3,4-dimethoxybenzylidene) cyclopentanone. Even though only (1E, 4E)-1,5-bis (3,4-dimethoxyphenyl) penta-1, 4-dien-3-one only interacting with the active site of Zn^{2+}, the His140, His141, Asp176, His178, Asp264, Asp176 and Tyr24 amino acids interacts through hydrogen bond. It exhibited about -10.27 kcal/mol of binding energy when it interacts

Table 2: Synthetic HDACi binding energy and interacting amino acids for HDAC1 and HDAC3

Name of the synthetic compound	Pubchem CID	Binding energy score (kcal/mol)		Hydrogen bonding between synthetic HDACi with protein interacting amino acids	
		HDAC1	HDAC3	HDAC1	HDAC3
AN-9	60748	-5.7	-6.14	O5-His140; O5-His178; O5-Asp264; O5-Zn; Zn-Asp170, Asp170; Zn-Asp264; Zn-His178; O10-Tyr303	O5-His135; O5-Asp170; O5-Zn; Zn-His172; O5-Asp170; Zn-Asp259; O6-Zn; o6-His135; O10-Tyr298
APHA	804603	-7.81	-7.12	O21-Ala136; O21-Arg34; O20-Arg34	O16-His135; O16-Asp170; O16-Zn; Zn-Asp170, Asp170; Zn-Asp259; Zn-His172
BML 210	9543540	-7.85	-8.72	N25-Ala136; N25-Gly137; N25-Gly300; N18-Gly138; O17-Gly138; O17-Gly260	O9-Asp259; O9-His172; 09-Zn; Zn-Asp170, Asp170; Zn-His172; N7-His172; O17-Tyr18
CBHA	5353484	-8.72	-8.41	O14-Asp176; O14-His178; O14-Zn; Zn- Asp176, Asp176; Zn-His178; Zn-Asp264; O10 Arg34; O8-Gly137	O14-His134; O14-His172; O14-Zn; Zn-His172; Zn-Asp170, Asp170; Zn-Asp259; O10-His172; N9-Tyr198
CI-994	2746	-7.48	-8.33	N20-Gly137; N20-Gly300; N13-Gly138; o12 Gly138; O12-His140; N4-Tyr303	O12-asp170; O12-Asp259; O12-Zn; Zn-Asp170, Asp170; Zn-Asp259; Zn-His172; N13-His172; N20-Tyr298; N4-Phe144
CRA024781	11749858	-9.99	-8.84	O29-Ala136; O29-Arg34; N28-Gly300; O15-Tyr303; O10-His140; O10-His141; O29-Ala136; O29-Arg34	O19-Zn; Zn-Asp170, Asp170; Zn-Asp259; O7-His172; O29-Arg28; O29-Gly295; O27-Gly132
CUDC101	11749858	-5.75	-6.59	O30-Arg270	O30-His135; O30-His134; O30-Asp170; O30-Asp259; O30-Zn; Zn-His172; Zn-Asp170, Asp170; Zn-Asp259
Dactinostat	6445533	-7.8	-8.68	O26-His140; O26-His141; O26-Asp176; O26-His178; O26-Zn; Zn-Asp176, Asp176; Zn-Asp264; Zn-His178	O26-His172; O26-Asp170; O26-Asp259; O26-Zn; Zn-Asp170, Asp170; Zn-Asp259; Zn-His172; N9-Ley266
IN-2001	6918714	-9.17	-9.79	N12-His178; N12-Tyr303; O11-Asp176; O11-Zn; Zn-Asp176, Asp176; Zn-Asp264; Zn-His178	O11-Asp170; O11-Asp259; 011-Zn; Zn-Asp170, Asp170; Zn-Asp259; Zn-His172; O23-Ala130
LBH-589	6918837	-8.41	-9.05	O24-Asp176; O24-Asp264; O24-His178; O24-Zn; Zn-Asp176, Asp176Zn-Asp264; Zn-His178	O24-His172; O24-Asp170, Asp170; O24-Zn; Zn-Asp170, Asp170; Zn-Asp259; Zn-His172;
Methotrexate	126941	-8.43	-5.59	O33-His178; O33-Asp264; O33-Zn; Zn-Asp170, Asp170; Zn-Asp264; Zn-His178; O32-Zn; O32-Tyr303	N15-Asp93; O33-Gly295, Gly295; O33-Asp93; O33-Tyr129; N24-gly295; o30-Asp93, Asp93; O32-Trp129
MGCD0103	9865515	-8.91	-9.86	O10-Gly300; O10-Arg34; N18-Tyr303; N27-Tyr204	N18-Asp93; N8-Tyr298; O10-Tyr298; N7-Asp170; O10-Zn; O10-His172Zn-Asp259; Zn-Asp170, Asp170
MS-275	4261	-9.37	-9.73	O20-His140; oO20-Asp176; O20-Asp264; O20-Zn; Zn-Asp176, Asp176; Zn-Asp264; Zn-His178	O20-Asp259; O20-His172; O20-Tyr298; O20-Zn; Zn-Asp170, Asp170; zn-Asp259; Zn-His172
Oxamflatin	5353852	-4.38	-4.92	O8-His140; O8-His141; N10-Asp176; O9-Tyr303; O10-Zn; Zn-Asp176; Zn-Asp264; Zn-His178	O8-His134; O8-His135; O8-Zn; Zn-Asp170, Asp170; Zn-Asp259; Zn-His172
Phenyl butyrate	5355254	-7.24	-7.55	O5-His140; O6-Asp176; O5-His178; O5-Zn; Zn-Asp176, Asp176; Zn-Asp264; Zn-His178	O5-Asp170, Asp170; O5-His172; O5-Zn; Zn-Asp170, Asp170; Zn-Asp259; Zn-His172; O6-Zn

Table 2: Continue

Name of the synthetic compound	Pubchem CID	Binding energy score (kcal/mol)		Hydrogen bonding between synthetic HDACi with protein interacting amino acids	
		HDAC1	HDAC3	HDAC1	HDAC3
PXD101	6918638	-9.74	-9.59	O22-Ala136; N7-Tyr303; O10-His141; O10-His178; O10-Zn; Zn-Asp264; Zn-Asp176, Asp176; Zn-His178	O9-Asp170; O9-Asp259; O9-His172; O9-Zn; Zn-Asp170, Asp170; Zn-Asp259; Zn-His172; N7-His172; O20-Tyr18
Pyroxamide	4996	-7.82	3.61	O9-Asp176; O9-Tyr303; O9-His178; O9-Zn; Zn-Asp176, Asp176; Zn-Asp264; Zn-His178	N5-Tyr298; O17-Gly295; O17-Gly131; O17-Trp129; N18-Trp129; O19-Arg28
SAHA	5311	-7.28	-7.86	O19-His178; O9-Asp176; O9-Asp264; O9-His178; O9-His140; O9-His141; O9-Zn; Zn-Asp176, Asp176; Zn-Asp264; Zn-His148	O9-His172; O9-Zn; Zn-Asp170, Asp170; Zn-Asp259; Zn-His172; O19-His172; N18-tyr198; O17-Tyr198
Scriptaid	5186	-8.26	-7.54	O11-Gly138; O8-Gly149; O24-His178	O22-His134; O22-Zn; Zn-Asp170, Asp170; Zn-Asp259; Zn-His17; N23-His172; N23-Tyr298; O24-Gly143
Suberic bis hydroxamate	5173	-7.43	-6.86	O6-Ala136; O12-His178; O12-His140; O12-Asp176; O12-Asp264; O12-Zn; Zn-Asp176, Asp176; Zn-Asp264; Zn-His178	O12-Asp170; O12-Asp259; O12-Zn; Zn-Asp170, Asp170; Zn-His172; Zn-Asp259; O8-His172
Trithio carbonates	292260	-6.3	-6.85	-	-
Triglitazone	5591	-9.37	-8.42	O28-Ala136; O25-Phe150; O15-Tyr303; O15-His141; O15-Zn; Zn-His178; Zn-Asp264; Zn-Asp176, Asp176	O15-His135; o15-Tyr298; O15-Zn; Zn-Asp170, Asp170; Zzn-Asp259; Zn-His172
Tubacin	6675804	-4.58	12.34	O33-Arg34; O33-Trp135; O23-Asp176; O23-His178; O23-Asp264; O23-Zn; Zn-Asp176, Asp176; Zn-His178; Zn-Asp264	O14-Leu266; N37-Asp93; O5-Tyr298; O33-Phe144; O33-Tyr18; N2-Tyr18; O23-Gly295

HDACi: Histone deacetylase inhibitor, HDAC1: Histone deacetylase 1, HDAC3: Histone deacetylase 3

Table 3: Molecular and bioactivity property measured for natural compounds

Name of the natural compound	Molecular property					Bioactivity property					
	LogP	TPSA	MW	n_{ON}	n_{OHNH}	GPCR	Ion Cha Mod	Kinase Inh	Nuc Rec Lig	Protease Inh	Enzyme Inh
Apicidin	3.41	138.84	623.80	11	3	0.1	-0.62	-0.4	-0.75	0.28	0.07
Azumamide A	0.86	159.49	513.64	10	6	0.29	-0.06	-0.11	-0.22	0.51	0.17
Azumamide D	0.08	159.49	485.59	10	6	0.3	0.05	-0.12	-0.13	0.47	0.17
Azumamide E	1.38	153.69	514.62	10	5	0.34	-0.01	-0.19	-0.1	0.52	0.23
Benzyl isoThiocyanate	3.01	12.36	137.00	1	0	-3.52	-2.89	-3.92	-3.99	-3	-2.94
Berberine	0.20	40.82	336.37	5	0	-0.11	0.71	-0.27	-0.78	-0.35	0.82
Chlamydocin	0.88	137.20	526.63	10	3	0.41	-0.08	-0.08	0.04	0.8	0.38
Curcumin	2.30	93.07	368.00	6	2	-0.06	-0.2	-0.26	0.12	-0.14	0.08
Dactinomycin	0.78	359.98	1255.44	28	6	-4.91	-5.32	-5.37	-5.41	-4.66	-5
Depudecin	0.20	65.51	212.25	4	2	-0.3	-0.03	-0.12	0	-0.16	0.6
Flavone	3.74	30.21	222.24	2	0	-0.3	-0.21	-0.12	-0.18	-0.52	0.03
HC-toxin	-1.06	137.20	436.51	10	3	0.31	-0.03	-0.1	0	0.75	0.37
Indolocarbazole	3.81	99.98	385.38	7	3	-0.07	-0.14	0.58	-0.26	-0.14	0.28
Largazole	1.96	7.77	478.81	2	0	0.17	-0.41	-0.61	-0.36	0.48	0.49
Linoleic acid	6.86	37.30	280.45	2	1	0.29	0.17	-0.16	0.31	0.12	0.38
Parthenolide	2.09	38.83	248.32	3	0	0.43	-0.07	-0.55	1.16	0.04	1.1
Pomiferin	5.24	100.13	420.46	6	3	0.1	-0.31	0.01	0.69	-0.24	0.47
Psammaplin A	3.43	163.84	664.40	10	6	0.09	-0.41	-0.22	0.08	-0.1	0.14
Romidepsin	1.60	142.70	540.71	10	4	0.26	-0.34	-0.47	-0.53	0.48	0.45
Stigmasterol	7.87	20.23	412.00	1	1	0.12	-0.08	-0.49	0.74	-0.02	0.53
Sulforaphane	1.15	29.44	177.29	2	0	-0.35	-0.59	-1.98	-0.84	-0.72	0.44
Thymoquinone	1.90	34.14	164.20	2	0	-1.4	-0.31	-1.27	-1.47	-1.44	-0.4
Trapoxin A	2.36	137.20	602.73	10	3	0.1	-0.58	-0.36	-0.43	0.45	-0.02
Trapoxin B	1.86	137.20	588.69	10	3	0.21	-0.43	-0.24	-0.15	0.59	0.08
Trichostatin A	2.68	69.64	302.37	5	2	0.05	-0.16	0.16	0.38	0.22	0.63

LogP: Logarithm of partition coefficient, TPSA: Total Polar Surface Area, MW: Molecular weight, n_{ON}: No. of Hydrogen bond acceptor, n_{OHNH}: No. of Hydrogen bond donor, GPCR: G protein-coupled receptor, Ion Cha Mod: Ion channel modulator, Kinase Inh: Kinase inhibitor, Nuc Rec Lig: Nuclear receptor ligand, Protease Inh: Protease inhibitor, Enzyme Inh: Enzyme inhibitor

Table 4: Molecular and Bioactivity property measured for synthetic compounds

Name of the synthetic compound	Molecular Property					Bioactive property					
	LogP	TPSA	MW	n_{ON}	n_{OHNH}	GPCR	Ion Cha Mod	Kinase Inh	Nuc Rec Lig	Protease Inh	Enzyme Inh
AN-9	2.86	52.61	202.25	4	0	-0.33	0.08	-0.57	-0.29	-0.22	0.04
APHA	1.58	79.29	284.32	5	2	0.13	0.01	-0.01	0.01	0.12	0.24
BML 210	3.92	84.22	339.44	5	4	-0.07	-0.15	0	-0.27	0.01	0.06
CBHA	0.31	98.65	222.20	6	4	-0.28	-0.53	0.15	-0.44	0.43	0.75
CI-994	1.48	84.22	269.30	5	4	-0.25	-0.32	-0.03	-0.61	-0.22	0.05
CRA024781	1.99	104.04	397.43	8	3	-0.01	-0.44	-0.01	-0.42	0.35	0.11
CUDC101	3.86	105.61	105.61	8	3	0.27	0.05	0.75	-0.07	0.3	0.53
Dactinostat	2.58	88.58	379.46	6	4	0.38	-0.06	0.42	0.07	0.45	0.51
IN-2001	2.15	81.66	339.40	6	3	0.08	-0.26	0.22	0.02	0.39	0.39
LBH-589	3.19	77.14	349.43	5	4	0.27	-0.11	0.27	-0.08	0.34	0.51
Methotrexate	-1.97	210.55	454.45	13	7	0.51	0.23	0.38	-0.38	0.27	0.72

Table 4: Continue

Name of the synthetic compound	Molecular Property					Bioactive property					
	LogP	TPSA	MW	n_{ON}	n_{OHNH}	GPCR	Ion Cha Mod	Kinase Inh	Nuc Rec Lig	Protease Inh	Enzyme Inh
MGCD0103	2.94	105.82	396.45	7	4	0.13	0.03	0.61	-0.18	-0.1	0.27
MS-275	2.03	106.35	376.42	7	4	0.23	0.21	0.29	-0.14	0.4	0.37
Oxamflatin	2.19	95.50	342.38	6	3	0.28	-0.06	0.27	0.45	0.72	0.71
Phenyl butyrate	2.19	26.31	204.27	2	0	-0.41	-0.05	-0.79	-0.27	-0.66	-0.06
PXD101	2.19	95.50	318.35	6	3	0	-0.45	-0.04	-0.02	0.42	0.42
Pyroxamide	1.40	91.32	265.31	6	3	0.03	-0.14	0.24	-0.41	0.48	0.52
SAHA	2.47	78.42	264.33	5	3	-0.07	-0.3	0.03	-0.39	0.42	0.4
Scriptaid Suberic	2.40	88.40	326.35	6	2	0.12	-0.33	0.09	-0.26	0.45	0.45
bishydroxamate	0.45	98.65	204.23	6	4	-0.33	-0.36	-0.31	-0.72	0.33	0.46
Trithiocarbonates	4.84	0.00	262.42	0	0	-0.5	-0.2	-0.56	-0.48	-0.52	0.1
Troglitazone	5.03	84.87	441.55	6	2	0.22	-0.48	-0.79	0.74	0.05	0.11
Tubacin	7.65	143.15	721.88	10	4	-1.02	-2.28	-1.46	-1.63	-0.49	-1

LogP: Logarithm of partition coefficient, TPSA: Total Polar Surface Area, MW: Molecular weight, n_{ON}: No. of Hydrogen bond acceptor, n_{OHNH}: No. of Hydrogen bond donor, GPCR: G protein-coupled receptor, Ion Cha Mod: Ion channel modulator, Kinase Inh: Kinase inhibitor, Nuc Rec Lig: Nuclear receptor ligand, Protease Inh: Protease inhibitor, Enzyme Inh: Enzyme inhibitor

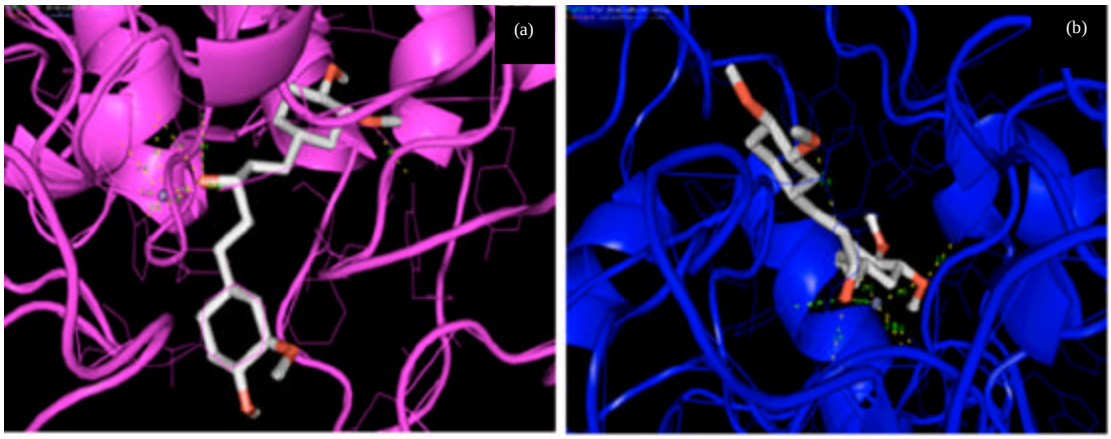

Fig. 4(a-b): (1E,4E)-1,5-bis (3,4-dimethoxyphenyl) penta-1,4-dien-3-one interact with histone deacetylase 1 (HDAC1) (a); (1E,4E)-1,5-bis (3,4-dimethoxyphenyl) penta-1,4-dien-3-one interact with histone deacetylase 3 (HDAC3) (b)

with HDAC3 amino acids His134, His135, Asp170, His172, Asp259, His172 and Arg28 were found as interacing through hydrogen bond. It contains twenty one carbon atoms, twenty two hydrogen atoms and five oxygen atoms, specifically the tenth carbonyl oxygen interacts with the active site of the Zn^{2+} ion by the distance of 1.9A° in both proteins (Fig. 4a, b), molecular properties such as LogP value 3.53, solubility-4.6, drug likeness 3.31 and drug score 0.71 which were well within the acceptable range. Remaining curcumin analogue compounds interaction with HDAC1 (Fig. 5) and HDAC3 (Fig. 6) were also given.

Table 5: Curcumin analogues binding energy and interacting amino acids for HDAC1 and HDAC3

IUPAC name of curcumin analogue	ChemBank ID	Binding energy score (kcal/mol)		Hydrogen bonding between curcumin analogue with protein interacting amino acids	
		HDAC1	HDAC3	HDAC1	HDAC3
1-(3, 4-dihydroxyphenyl)-7 -(4-hydroxy-3-methoxyphenyl) hepta-1, 6-diene-3, 5-dione	3558654	-10	-8.16	O9-His141; 09-His178; O9-Asp264; O9-Zn-Asp176, Asp176; Zn-His178; Zn-Asp264; O12-His140	O9-His134;O12-His134; O12-His172 O12-Asp259; O12-Asp176; O12-ZnZn-Asp176, Asp176; Zn-Asp259; Zn-His172
1, 7-bis(4-hydroxy-3-methoxyphenyl) hepta-1, 6-diene-3, 5-dione	2081006	-7.56	-9.98	O27-Ala136; O9-His140; O12-His178; O12 Gly300; O12-Asp264; O12-Zn; Zn-Asp176, Asp176; Zn-Asp264; Zn-His178	O2-Arg28; O9-His134 O9-Asp170; O9-Zn O12-Asp259; O12-His172; O12-Zn; Zn-Asp170, Asp170; Zn-Asp259
1E, 6E)-1, 7-bis(4-hydroxy-3, 5-dimethoxyphenyl)hepta-1, 6-diene-3, 5-dione	2113465	-7.69	-8	O12-Tyr303; O9-His141; O9-His178; O9-Asp264; O9-Zn; Zn-Asp264; Zn-His178; Zn-Asp176, Asp176	O12-Tyr298; O9-His134; O10-His135; O9-His172; O9-Zn; Zn-Asp170, Asp170; Zn-His172
(1E, 6E)-1-(3-hydroxy-2-methoxyphenyl) -7-(3-hydroxy-4-methoxyphenyl) hepta-1, 6-diene-3, 5-dione	3001893	-7.93	-7.02	O10-His178; O10-Tyr303; O10-Zn; Zn-Asp176, Asp176; Zn-His178; Zn-Asp264; O13-Tyr303; O23-His178	O23-Arg28; O10-His135; O10-His172; O10-His134; O10-Asp170; O10-Zn; Zn-Asp170, Asp170; Zn-Asp259; Zn-His172; O13-Gly143
1, 7-bis(4-methoxyphenyl)hepta-1, 6-diene-3, 5-dione	2099406	-7.99	-8.21	O13-Tyr303; O10-Gly138; O10-His140; O10-Gln260	O13-His135; O13-His172; O13-Asp259; O13-Asp170; O13-Zn; Zn-Asp170, Asp170; Zn-His172; Zn-Asp259
1, 7-bis(1, 3-benzodioxol-5-yl)hepta-1, 6-diene-3, 5-dione	2099407	-7.94	-7.41	O5-Asp176; O1-His141; O1-His178; O1-Zn; Zn-Asp264; Zn-His178; Zn-Asp176; O14-Arg34, Arg34	O1-His135; O1-Asp170; O1-His172; O1-Asp170; O1-Zn; Zn-Asp170, Asp170; Zn-Asp259; Zn-His172; O5-Gly143
1-(3, 4-dimethoxyphenyl)-4, 4-dimethylpent-1-en-3-one	2091339	-6.61	-8.16	O10-His141; O10-Asp176; O10-Asp264; O10-His178; O10-Zn; Zn-His178; Zn-Asp264; Zn-Asp176, Asp176	O10-His134; O10-Asp170; O10-His172; O10-Zn; Zn-Asp170, Asp170; Zn-His178; Zn-Asp259
(2E, 6E)-2, 6-bis(3, 4-dimethoxybenzylidene) cyclohexanone	1926852	-8.08	-8.08	O25-Gly149; O25-Tyr303; O28-Tyr24	-
(2E, 6E)-2, 6-bis(4-hydroxy-3-methoxybenzylidene) cyclohexanone	1797887	-8.11	-7.27	O23-Gly148; O23-Tyr303; O27-Tyr24; O2-Arg34, Arg34	O17-Gly132; O27-Leu266
(3E)-4-(3, 4-dimethoxyphenyl) but-3-en-2-one	2119938	-6.78	-6.73	O10-His140; O10-His141; O10-Asp176; O10-His178; O10-Asp176; O10-Asp264; O10-Zn; Zn-Asp264; Zn-Asp176, Asp176; Zn-His178; O14-Tyr24	O10-His134; O10-His135; O10-Asp170; O10-His172; O10-Zn; Zn-Asp170, Asp170; Zn-His172; Zn-Asp259
(1E, 4E)-1, 5-bis(3, 4-dimethoxyphenyl)penta-1, 4-dien-3-one	1916824	-10.20	-10.27	O10-His140; O10-His141; O10-Asp176; O10-His178; O10-Zn Zn-His178 Zn-Asp264 Zn-Asp176, Asp176 O25-Tyr24	O10-His134; O10-His135; O10-Asp170; O10-Zn; Zn-Asp170, Asp170; Zn-His172; Zn-Asp259; O10-His172
(2E)-2-(3, 4, 5-trimethoxybenzylidene) cyclohexanone	2075223	-6.67	-5.49	O13-Gly136; O2-Arg34	O13-His172; O13-Tyr198; O2-Phe199
(2E, 5E)-2, 5-bis(3, 4-dimethoxybenzylidene) cyclopentanone	2071111	-7.42	-7.98	O27-Cys151; O24-Gly149	-

HDACi: Histone deacetylase inhibitor, HDAC1: Histone deacetylase 1, HDAC3: Histone deacetylase 3

Table 6: Molecular and bioactivity property measured for curcumin analogue compounds

	Molecular property			Bioactive property							
IUPAC name of curcumin analogue	Log P	TPSA	MW	n_{ON}	n_{OHNH}	GPCR	Ion Cha Mod	Kinase Inh	Nuc Rec Lig	Protease Inh	Enzyme Inh
1-(3, 4-dihydroxyphenyl)-7-(4-hydroxy-3-methoxyphenyl)hepta-1, 6-diene-3, 5-dione	1.995	104.06	354	6	3	-0.06	-0.21	-0.27	0.13	-0.14	0.08
1, 7-bis(4-hydroxy-3-methoxyphenyl)hepta-1,6-diene-3, 5-dione	2.303	93.066	368	6	2	-0.06	-0.2	-0.26	0.12	-0.14	0.08
1E, 6E)-1, 7-bis(4-hydroxy-3, 5-dimethoxyphenyl) hepta-1, 6-diene-3, 5-dione	2.335	111.53	428	8	2	-0.07	-0.18	-0.22	0.08	-0.11	0.09
(1E, 6E)-1-(3-hydroxy-2-methoxyphenyl)-7-(3-hydroxy-4-methoxyphenyl)hepta-1, 6-diene-3, 5-dione	2.296	93.066	368	6	2	-0.07	-0.23	-0.31	0.09	-0.18	0.04
1, 7-bis(4-methoxyphenyl)hepta-1, 6-diene-3, 5-dione	3.738	52.61	336	4	0	-0.08	-0.24	-0.32	0.08	-0.12	0.03
1, 7-bis(1, 3-benzodioxol-5-yl)hepta-1, 6-diene-3, 5-dione	3.405	71.078	364	6	0	-0.05	-0.25	-0.32	0.02	-0.12	0.04
1-(3, 4-dimethoxyphenyl)-4, 4-dimethylpent-1-en-3-one	3.182	35.539	248	3	0	-0.34	-0.43	-0.73	-0.34	-0.49	-0.01
(2E, 6E)-2, 6-bis(3, 4-dimethoxybenzylidene)cyclohexanone	4.261	54.007	394	5	0	-0.12	-0.27	-0.32	-0.09	-0.08	-0.03
(2E, 6E)-2, 6-bis(4-hydroxy-3-methoxybenzylidene) cyclohexanone	3.646	75.995	366	5	2	-0.1	-0.25	-0.31	-0.02	-0.08	0.02
(3E)-4-(3, 4-dimethoxyphenyl) but-3-en-2-one	1.856	35.539	206	3	0	-0.75	-0.55	-0.94	-0.72	-0.83	-0.25
(1E, 4E)-1, 5-bis(3, 4-dimethoxyphenyl) penta-1, 4-dien-3-one	3.477	54.007	354	5	0	-0.1	-0.28	-0.16	0	-0.09	0
(2E)-2-(3, 4, 5-trimethoxybenzylidene) cyclohexanone	2.815	44.773	276	4	0	-0.1	-0.28	-0.16	0	-0.09	0
(2E, 5E)-2, 5-bis(3, 4-dimethoxybenzylidene)cyclopentanone	3.756	54.007	380	5	0	-0.28	-0.23	-0.34	-0.06	-0.11	-0.03

LogP: Logarithm of partition coefficient, TPSA: Total polar surface area, MW: Molecular weight, N_{ON}: No. of hydrogen bond acceptor, n_{OHNH}: No. of Hydrogen bond donor, GPCR: G protein-coupled receptor, Ion Cha Mod: Ion channel modulator, Kinase Inh: Kinase inhibitor, Nuc Rec Lig: Nuclear receptor ligand, Protease Inh: Protease inhibitor, Enzyme Inh: Enzyme inhibitor

Table 7: Solubility, Drug likeness and Drug score for Curcumin and curcumin analogues

Curcumin and IUPAC Name of curcumin analogue	Solubility	Drug likeness	Drug score
Curcumin	-3.62	-3.95	0.39
1-(3, 4-dihydroxyphenyl)-7-(4-hydroxy-3-methoxyphenyl)hepta-1, 6- diene-3, 5-dione	-3.31	-3.27	0.42
1, 7-bis(4-hydroxy-3-methoxyphenyl)hepta-1, 6-diene-3, 5-dione	-3.62	-3.95	0.39
(1E, 6E)-1, 7-bis(4-hydroxy-3, 5-dimethoxyphenyl)hepta-1, 6-diene-3, 5-dione	-3.66	-3.13	0.38
(1E, 6E)-1-(3-hydroxy-2-methoxyphenyl)-7-(3-hydroxy-4-methoxyphenyl)hepta-1, 6-diene-3, 5-dione	-3.62	-3.14	0.4
1, 7-bis(4-methoxyphenyl)hepta-1, 6-diene-3, 5-dione	-4.21	-4.42	0.36
1, 7-bis(1, 3-benzodioxol-5-yl)hepta-1, 6-diene-3, 5-dione	-5.6	-4.14	0.27
1-(3, 4-dimethoxyphenyl)-4, 4-dimethylpent-1-en-3-one	-3.09	-3.62	0.43
(2E, 6E)-2, 6-bis(3, 4-dimethoxybenzylidene)cyclohexanone	-4.66	0.51	0.46
(2E, 6E)-2, 6-bis(4-hydroxy-3-methoxybenzylidene)cyclohexanone	-4.03	-1.25	0.41
(3E)-4-(3, 4-dimethoxyphenyl)but-3-en-2-one	-2.48	-0.07	0.44
(1E, 4E)-1, 5-bis(3, 4-dimethoxyphenyl)penta-1, 4-dien-3-one	-4.06	3.31	0.71
2E)-2-(3, 4, 5-trimethoxybenzylidene)cyclohexanone	-3.25	-3.66	0.43
(2E, 5E)-2, 5-bis(3, 4-dimethoxybenzylidene)cyclopentanone	-4.39	2.39	0.59

DISCUSSION

Virtual screening is now became an alternative drug development strategy for many challenging areas including cancer drug development. The vast array of natural and synthetic products demonstrating the anticancer activity against tumor cell lines demands computational screening for rapid identification and development of potential therapeutic leads. Hence, worldwide pharmaceutical industries are investing torrential in virtual screening technologies. As suggested (Lipinski *et al*., 2001), the current trend of carrying out lead optimization for selecting the compound or compounds with the greatest potential to be developed into safe and effective medicines was applied in this research. HDACi have been shown to bind directly to the HDAC active site and thereby inhibits deacetylation through blocking substrate access. A wide range of structures has been shown to inhibit the Class I/II HDAC enzyme activity. Almost all HDAC inhibitors have a common characteristic pharmacophore including of a metal binding domain, a linker domain and a surface recognition domain (Noureen *et al*., 2010). Hence, general pharmacophore having these characteristics can be proposed for the HDAC inhibitors. Already several Zn^{2+} dependent HDACi classified as short-chain fatty acid, hydroxamic acid, benzamide and cyclic tetra peptides are well known. The Food and Drug Administration (FDA) approval given to SAHA and romidepsin validates the prospects of HDACi as anticancer therapeutics (Chou *et al*., 2011).

The natural compound repository by virtue of their vast array of chemical diversity and unique properties could continue to act as a promising source for developing new-targeted anticancer agents. As a part of this study continuing effort to identify novel breast cancer implicated HDAC1 and HDAC3 inhibitors, a panel of small molecules including both natural and synthetic compounds were virtually screened. Natural compounds likes the *Curcuma longa* plant derivative curcumin (Akram *et al*., 2010) and *Streptomyces hygroscopicus* metabolite TSA (Izawa *et al*., 2009) has shown high molecular interaction with the modeled breast cancer specific HDAC1 and HDAC3. Earlier attempts to determine the relationship between the structure information and the breast cancer implicated HDAC inhibitory potency was scarce in the literature. The analysis of the best docked ligands allowed knowing the likely binding mode of these HDACi compounds and their possible role

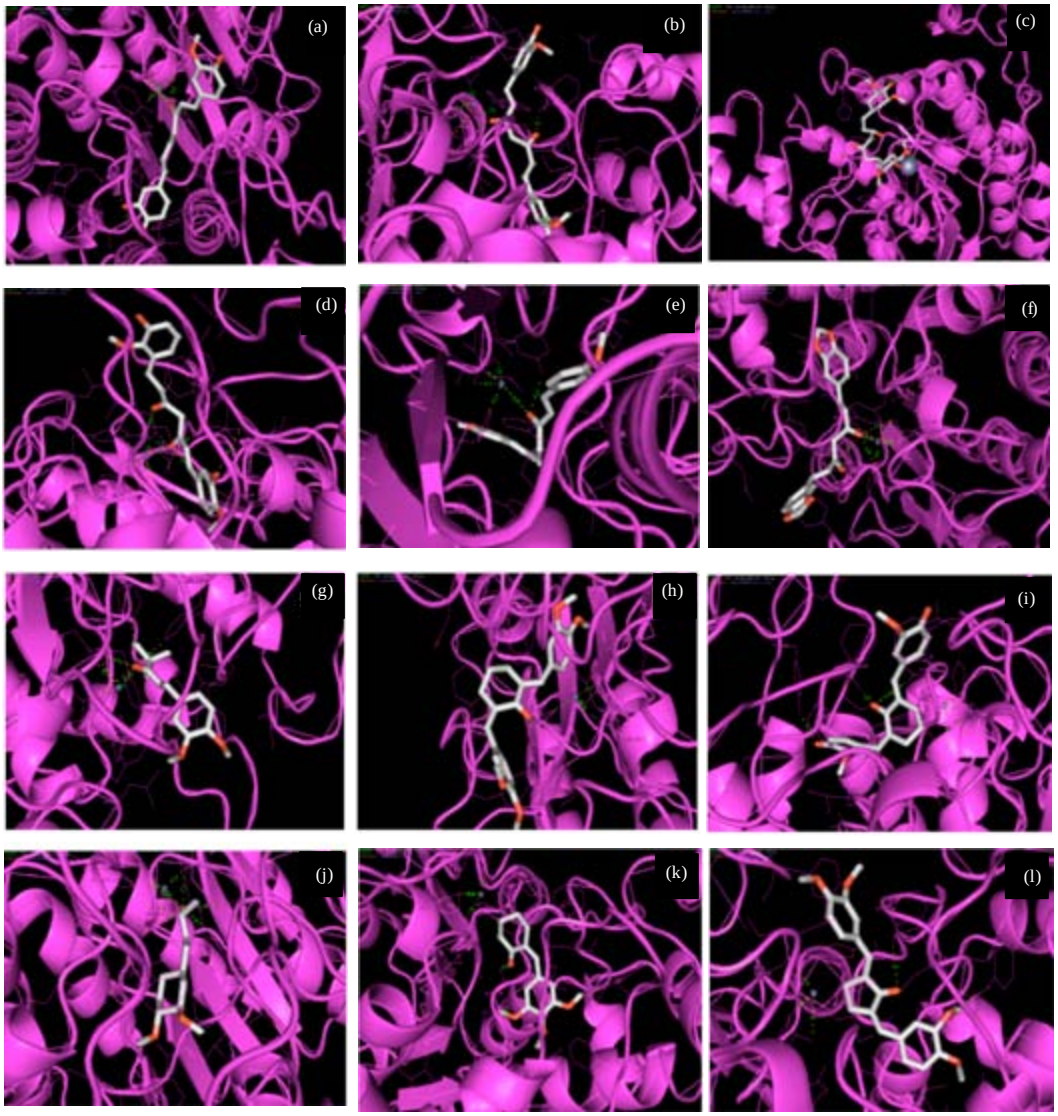

Fig. 5(a-l): Curcumin analogues interact with histone deacetylase 1 (HDAC1) protein, 1-(3,4-dihydroxyphenyl)-7-(4-hydroxy-3-methoxyphenyl)hepta-1,6-diene-3,5-dione (a); 1,7-bis(4-hydroxy-3-methoxyphenyl)hepta-1,6-diene-3,5-dione (b); (1E,6E)-1,7-bis(4-hydroxy-3,5-dimethoxyphenyl)hepta-1,6-diene-3,5-dione (c); 1E,6E)-1-(3-hydroxy-2-methoxyphenyl)-7-(3-hydroxy-4-methoxyphenyl) hepta-1,6-diene-3,5-dione (d); 1,7-bis(4-methoxyphenyl)hepta-1,6-diene-3,5-dione (e); 1,7-bis(1,3-benzodioxol-5-yl)hepta-1,6-diene-3,5-dione (f); 1-(3,4-dimethoxyphenyl)-4,4-dimethylpent-1-en-3-on (g); (2E,6E)-2,6-bis(3,4-dimethoxybenzylidene) cyclohexanone (h); (2E,6E)-2,6-bis(4-hydroxy-3-methoxybenzylidene) cyclohexanone (i); ((3E)-4-(3,4-dimethoxyphenyl)but-3-en-2-on (j); (2E)-2-(3,4,5-trimethoxybenzylidene) cyclohexanone (k); (2E,5E)-2,5-bis(3,4-dimethoxybenzylidene) cyclopentanone (l)

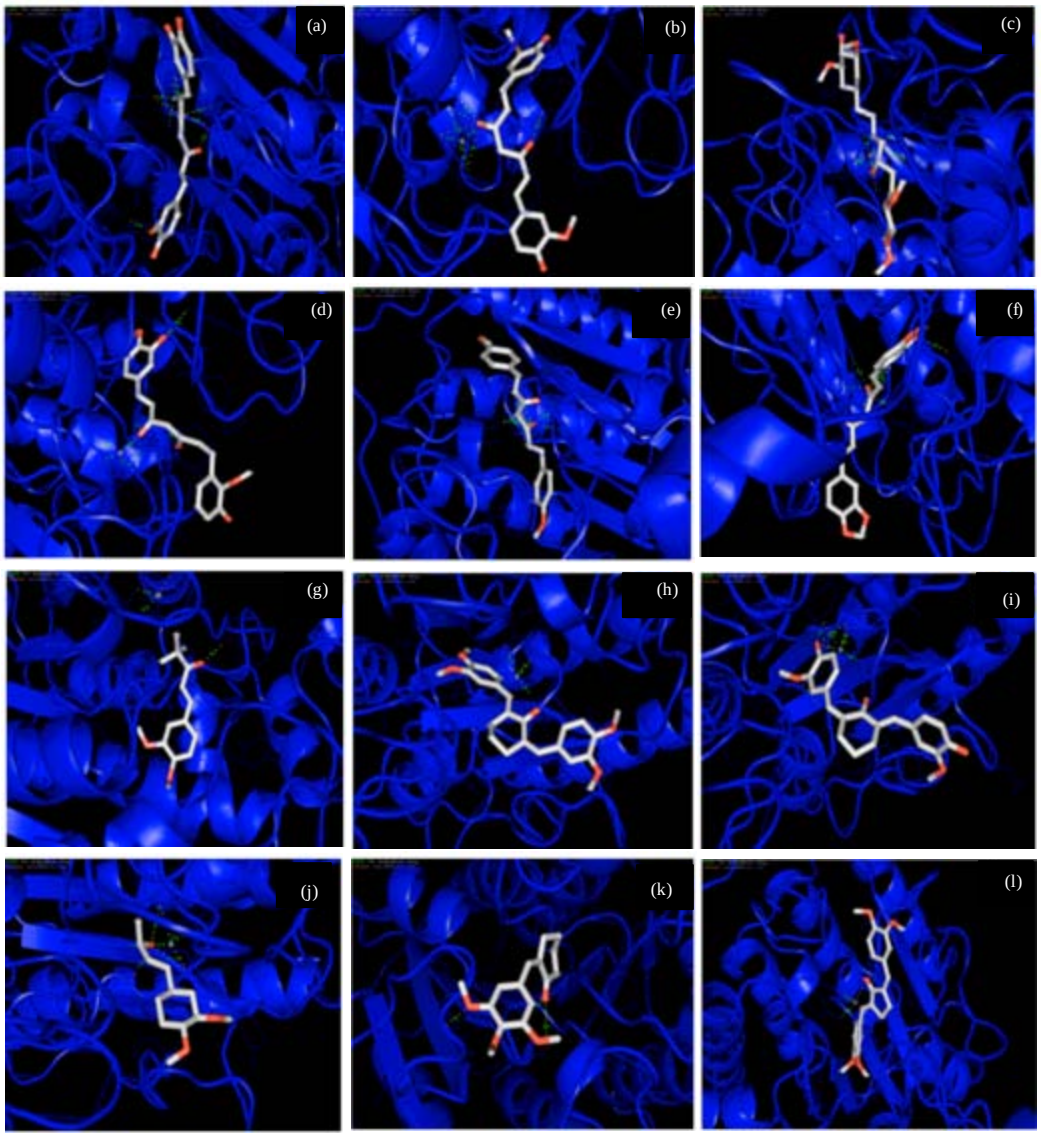

Fig. 6(a-l): Curcumin analogues interact with histone deacetylase 3 (HDAC3) protein, 1-(3,4-dihydroxyphenyl)-7-(4-hydroxy-3-methoxyphenyl)hepta-1,6-diene-3,5-dione (a); 1,7-bis(4-hydroxy-3-methoxyphenyl)hepta-1,6-diene-3,5-dione (b); (1E,6E)-1,7-bis(4-hydroxy-3,5-dimethoxyphenyl)hepta-1,6-diene-3,5-dione (c);1E,6E)-1-(3-hydroxy-2-methoxyphenyl)-7-(3-hydroxy-4-methoxyphenyl) hepta-1,6-diene-3,5-dione (d) ; 1,7-bis(4-methoxyphenyl)hepta-1,6-diene-3,5-dione (e); 1,7-bis(1,3-benzodioxol-5-yl)hepta-1,6-diene-3,5-dione (f);1-(3,4-dimethoxyphenyl)-4,4-dimethylpent-1-en-3-on (g); (2E,6E)-2,6-bis(3,4-dimethoxybenzylidene) cyclohexanone (h); (2E,6E)-2,6-bis(4-hydroxy-3-methoxybenzylidene) cyclohexanone (i); ((3E)-4-(3,4-dimethoxyphenyl)but-3-en-2-on (j); (2E)-2-(3,4,5-trimethoxybenzylidene) cyclohexanone (k); (2E,5E)-2,5-bis(3,4-dimethoxybenzylidene) cyclopentanone (l)

as chemo preventive agent. Binding energies of the drug-enzyme (receptor) interactions are important to describe their fitness to bind with the target macromolecule. The obtained results were useful to understand the structural features required to enhance the inhibitory activities (Phosrithong and Ungwitayatorn, 2010).

Although curcumin is known as non-toxic, anti-inflammatory and anti-cancer active agent, the preclinical as well as clinical studies indicated their poor bioavailability and pharmacokinetic profiles, limiting its application in anti-cancer therapies. Though many synthetic modifications of curcumin aimed at their bioactivity enhancement were intensively studied, only a few focused on the pharmacokinetic profile improvement (Tsai *et al*., 2011; Reuter *et al*., 2011). Even though the anti carcinogenic property of curcumin is known, the exact mechanism of its action or the identity of the target receptor is not completely understood till yet (Chakraborti *et al*., 2011). The present prediction information on curcumin breast cancer HDACi activity would provide a novel lead for breast cancer research. During drug design, more than a few factors including the normal "drug-like" and Absorption, Distribution, Metabolism and Excretion (ADME) concerns have to be taken into consideration to reduce late-stage attrition (Tambunan and Wulandari, 2010). Therefore, the present study, ADME parameters were calculated according to the Lipinski's "rule of five."

Synergistic combining of molecular docking with pharmacophore modeling based breast cancer targeting HDACi identification has not been studied earlier. Although HDAC1 and HDAC3 shares some structural and functional similarities with other class I HDACs, it exists in multi subunit complexes separate and different from other known HDAC complexes, implying that HDACs might function in a distinct manner (Yang *et al*., 2002). Hence, the potentiality of breast cancer specific HDACi targeting regulation of their global gene expression by epigenetic modification would offer potential anticancer therapeutic leads.

CONCLUSION

The HDAC1 and HDAC3 proteins play major role in breast cancer, both protein structures were modeled and the PROCHECK result showed reliability of the proteins. Based on virtual screening result curcumin has best compound for both proteins but it has poor drug likeness property, to overcome this problem to further study the curcumin analogue compounds. Based on this study (1E, 4E) -1,5-bis (3,4-dimethoxyphenyl) penta-1,4-dien-3-one was predicted as a potential lead drug-like molecule that selectively inhibits HDAC1 and HDAC3. The lead active analogue compound suggested as novel feature candidate may serve as useful leads for breast cancer therapeutic intervention study.

ACKNOWLEDGMENT

We sincerely thanks the management of AU-KBC Research Centre, Anna University, for providing necessary facilities to carry out this study.

REFERENCES

Akram, M., Shahab-Uddin, A. Ahmed, K. Usmanghani, A. Hannan, E. Mohiuddin and M. Asif, 2010. *Curcuma longa* and curcumin: A review article. Romanian J. Biol. Plant Biol., 55: 65-70.

Alteri, R., P. Bandi, L. Brinton, C. Casares and V. Cokkinides *et al*., 2011. Breast cancer facts and figures 2011-2012. American Cancer Society, Atlanta, GA., USA., pp: 1-36.

Binkowski, T.A., S. Naghibzadeh and J. Liang, 2003. CASTp computed atlas of surface topography of proteins. Nucleic Acid Res., 31: 3352-3355.

Chakraborti, S., L. Das, N. Kapoor, A. Das and V. Dwivedi *et al.*, 2011. Curcumin recognizes a unique binding site of tubulin. J. Med. Chem., 54: 6183-6196.

Chou, C.W., M.S. Wu, W.C. Huang and C.C. Chen, 2011. HDAC inhibition decreases the expression of EGFR in colorectal cancer cells. PLoS ONE, Vol. 6, No. 3. 10.1371/journal.pone.0018087

Duong, V., C. Bret, L. Altucci, A. Mai and C. Duraffourd *et al.*, 2008. Specific activity of class II histone deacetylases in human breast cancer cells. Mol. Cancer Res., 6: 1908-1919.

Dworkin, A.M., T.H.M. Huang and A.E. Toland, 2009. Epigenetic alterations in the breast: Implications for breast cancer detection, prognosis and treatment. Semin. Cancer Biol., 19: 165-171.

Ertl, P., 2012. Database of bioactive ring systems with calculated properties and its use in bioisosteric design and scaffold hopping. Bioorg. Med. Chem., 20: 5436-5442.

Friedrich, A., R. Ripp, N. Garnier, E. Bettler, G. Deleage, O. Poch and L. Moulinier, 2007. Blast sampling for structural and functional analyses. BMC Bioinform., Vol. 8. 10.1186/1471-2105-8-62

Geer, L.Y., A. Marchler-Bauer, R.C. Geer, L. Han and J. He *et al.*, 2010. The NCBI biosystems database. Nucleic Acids Res., 38: D492-D496.

Izawa, M., O. Takekawa, T. Arie, T. Teraoka, M. Yoshida, M. Kimura and T. Kamakura, 2009. Inhibition of histone deacetylase causes reduction of appressorium formation in the rice blast fungus *Magnaporthe oryzae*. J. Gen. Applied Microbiol., 55: 489-498.

Jemal, A., F. Bray, M.M. Center, J. Ferlay, E. Ward and D. Forman, 2011. Global cancer statistics. CA: Cancer J. Clin., 61: 69-90.

Krusche, C.A., P. Wulfing, C. Kersting, A. Vloet and W. Bocker *et al.*, 2005. Histone deacetylase-1 and -3 protein expression in human breast cancer: A tissue microarray analysis. Breast Cancer Res. Treat., 90: 15-23.

Laskowski, R.A., M.W. MacArthur, D.S. Moss and J.M. Thornton, 1993. PROCHECK: A program to check the stereochemical quality of protein structures. J. Applied Cryst., 26: 283-291.

Li, Q., T. Cheng, Y. Wang and S.H. Bryant, 2010. PubChem as a public resource for drug discovery. Drug Discovery Today, 15: 1052-1057.

Lipinski, C.A., F. Lombardo, B.W. Dominy and P.J. Feeney, 2001. Experimental and computational approaches to estimate solubility and permeability in drug discovery and development settings. Adv. Drug Del. Rev., 46: 3-26.

Lustberg, M.B. and B. Ramaswamy, 2011. Epigenetic therapy in breast cancer. Curr. Breast Cancer Rep., 3: 34-43.

Mariotto, A.B., K.R. Yabroff, Y. Shao, E.J. Feuer and M.L. Brown, 2011. Projections of the cost of cancer care in the United States: 2010-2020. J. Natl. Cancer Inst., 103: 117-128.

Morris, G.M., D.S. Goodsell, R.S. Halliday, R. Huey, W.E. Hart, R.K. Belew and A.J. Olson, 1998. Automated docking using a lamarckian genetic algorithm and empirical binding free energy function. J. Computat. Chem., 19: 1639-1662.

Noureen, N., S. Kalsoom and H. Rashid, 2010. Ligand based pharmacophore modelling of anticancer histone deacetylase inhibitors. Afr. J. Biotechnol., 9: 3923-3931.

Osterberg, T. and U. Norinder, 2001. Prediction of drug transport processes using simple parameters and PLS statistics: The use of ACD/logP and ACD/ChemSketch descriptors. Eur. J. Pharm. Sci., 12: 327-337.

Oyama, T., Y. Yasui and T. Tanaka, 2009. Breast cancer chemoprevention: Current perspectives. Curr. Enzyme Inhib., 5: 198-208.

Paramasivan, M., G. Sankaran, N. Sethuraman, D.S. Devadoss, S. Thangavelu and M. Gangatharan, 2011. Molecular modelling of urease accessory interaction proteins of *Helicobacter pylori* J 99 and predicting an interruption in interaction by *Vigna radiata* Defensins. Bioinformation, 5: 410-415.

Phosrithong, N. and J. Ungwitayatorn, 2010. Molecular docking study on anticancer activity of plant-derived natural products. Med. Chem. Res., 19: 817-835.

Reuter, S., Gupta, S.C., B. Park, A. Goel and B.B. Aggarwal, 2011. Epigenetic changes induced by curcumin and other natural compounds. Genes Nutr., 6: 93-108.

Seeliger, D. and B.L. de Groot, 2010. Ligand docking and binding site analysis with PyMOL and Autodock/Vina. J. Comput. Aided Mol. Des., 24: 417-422.

Seiler, K.P., G.A. George, M.P. Happ, N.E. Bodycombe and H.A. Carrinski *et al.*, 2008. ChemBank: A small-molecule screening and cheminformatics resource database. Nucleic Acids Res., 36: D351-D359.

Subha, K. and G.R. Kumar, 2008. Assessment for the identification of better HDAC inhibitor class through binding energy calculations and descriptor analysis. Bioinformation, 3: 218-222.

Tambunan, U.S.F. and E.K. Wulandari, 2010. Identification of a better Homo sapiens class II HDAC inhibitor through binding energy calculations and descriptor analysis. Bio Med. Cent. Bioinform., Vol. 11, 10.1186/1471-2105-11-S7-S16

Tsai, Y.M., C.F. Chien, L.C. Lin and T.H. Tsai, 2011. Curcumin and its nano-formulation: The kinetics of tissue distribution and blood-brain barrier penetration. Int. J. Pharm., 416: 331-338.

Wishart, D.S., C. Knox, A.C. Guo, D. Cheng and S. Shrivastava *et al.*, 2008. DrugBank: A knowledgebase for drugs, drug actions and drug targets. Nucleic Acids Res., 36: D901-D906.

Yang, W.M., S.C. Tsai, Y.D. Wen, G. Fejer and E. Seto, 2002. Functional domains of histone deacetylase-3. J. Biol. Chem., 277: 9447-9454.